

T.P. Wagner · T.L. Grove

Melt/harzburgite reaction in the petrogenesis of tholeiitic magma from Kilauea volcano, Hawaii

Received: 4 February 1997 / Accepted: 27 August 1997

Abstract We use the results of elevated pressure melting experiments to constrain the role of melt/mantle reaction in the formation of tholeiitic magma from Kilauea volcano, Hawaii. Trace element abundance data is commonly interpreted as evidence that Kilauea tholeiite is produced by partial melting of garnet lherzolite. We experimentally determine the liquidus relations of a tightly constrained estimate of primary tholeiite composition, and find that it is not in equilibrium on its liquidus with a garnet lherzolite assemblage at any pressure. The composition is, however, cosaturated on its liquidus with olivine and orthopyroxene at 1.4 GPa and 1425 °C, from which we infer that primary tholeiite is in equilibrium with harzburgite at lithospheric depths beneath Kilauea. These results are consistent with our observation that tholeiite primary magmas have higher normative silica contents than experimentally produced melts of garnet lherzolite. A model is presented whereby primary tholeiite forms via a two-stage process. In the first stage, magmas are generated by melting of garnet lherzolite in a mantle plume. In the second stage, the ascent and decompression of magmas causes them to react with harzburgite in the mantle by assimilating orthopyroxene and crystallizing olivine. This reaction can produce typical tholeiite primary magmas from significantly less siliceous garnet lherzolite melts, and is consistent with the shift in liquidus boundaries that accompanies decompression of an ascending magma. We determine the proportion of reactants by major element mass balance. The ratio of mass assimilated to mass crystallized (M_a/M_c) varies from 2.7 to 1.4, depending on the primary

magma composition. We use an AFC calculation to model the effect of melt/harzburgite reaction on melt rare earth and high field strength element abundances, and find that reaction dilutes, but does not significantly fractionate, the abundances of these elements. Assuming olivine and orthopyroxene have similar heats of fusion, the M_a/M_c ratio indicates that reaction is endothermic. The additional thermal energy is supplied by the melt, which becomes superheated during adiabatic ascent and can provide more thermal energy than required. Melt/harzburgite reaction likely occurs over a range of depths, and we infer a mean depth of 42 km from our experimental results. This depth is well within the lithosphere beneath Kilauea. Since geochemical evidence indicates that melt/harzburgite reaction likely occurs in the top of the Hawaiian plume, the plume must be able to thin a significant portion of the lithosphere.

Introduction

Tholeiitic basalt is the most abundant magma type erupted at Kilauea volcano, Hawaii and comprises over 95% of other Hawaiian volcanoes (Clague and Dalrymple 1987). Understanding the origin of Kilauea tholeiite thus provides insight into the most frequent magma forming events at the Hawaiian hotspot, and is an important step in understanding hotspot magma generation overall. Variation in the trace element abundances of Kilauea tholeiite implies that tholeiite is produced by low-degree partial melting of garnet lherzolite (e.g. Hofmann et al. 1984; Budahn and Schmitt 1985). This result is consistent with geophysical models of the Hawaiian plume, which indicate that melting begins within the garnet stability field (Liu and Chase 1989, 1991; Watson and McKenzie 1991). Experimental studies, however, show that estimated primary and primitive tholeiites are not in equilibrium with garnet lherzolite at any pressure, but are in equilibrium with more refractory harzburgite at lithospheric depths beneath Kilauea (Green and Ringwood 1967; Green 1970; Eggins 1992a). Eggins

T.P. Wagner (✉)¹ · T.L. Grove
Department of Earth, Atmospheric and Planetary Science,
Massachusetts Institute of Technology, Cambridge,
MA 02139, USA

Present address: ¹Department of Geology,
University of Papua New Guinea, Box 414 University PO, NCD,
Papua New Guinea, e-mail: 100253.1545@compuserve.com

Editorial responsibility: J. Hoefs

(1992b) showed that magmas with trace element evidence of a garnet lherzolite source and experimental or major element evidence of equilibrium with harzburgite cannot be produced solely by melting of an upwelling plume. Eggins concluded that plume-derived garnet lherzolite melts must equilibrate with harzburgite during ascent in order to become tholeiite primary magmas, but did not propose a mechanism by which equilibration could occur. Herein, we evaluate the role of melt/harzburgite interaction in the petrogenesis of Kilauea tholeiite, and develop a reaction mechanism within a conceptual framework of melt/mantle reaction (Kelemen 1990; Kelemen et al. 1990a). We calculate compositional, thermal, and mass constraints on reaction using the results of an experimental melting study.

Experimental and analytical methods

Starting material

The starting material for the experiments (Table 1) is an estimate of primary Kilauea tholeiite composition based on picritic glasses submarine-erupted from Kilauea's eastern rift zone (Clague et al. 1991). These glasses contain up to 15.0 wt% MgO, and are the most magnesian glasses found in Hawaii (Frey 1991). The glasses have undergone only minor modification since segregation from the mantle. Clague et al. (1991) accounted for this modification and calculated the primary magma composition using linear regression. This calculation was later refined by Clague et al. (1995), who reported a minor error in their 1991 calculation, and calculated both high- and low-FeO primary magma endmembers. Fortunately, the 1991 primary magma composition is similar to the average 1995 composition (Table 1).

The picritic glasses are a better choice for estimating primary tholeiite composition than the subaerial lavas generally used (review in Eggins, 1992a). As glasses, these samples definitely represent liquid compositions. Equally magnesian subaerial lavas typically have accumulated olivine phenocrysts, and are not representative of liquids. Furthermore, the glasses are almost in Fe/Mg exchange equilibrium with mantle olivine, which indicates that the glass magmas escaped much of the shallow level processing that affects subaerially erupted magmas. This processing involves crystal fractionation, crystal entrainment, magma mixing and assimilation. These processes strongly fractionate major element concentrations, and add uncertainty to calculations of primary magma composition. Estimates of tholeiite primary magma composition based on subaerial lavas that employ olivine addition or regression techniques (e.g. Murata and Richter 1966; Maaloe 1979; Eggins 1992a) have lower MgO and SiO₂ and higher Al₂O₃, CaO and TiO₂ concentrations than the picritic glass based estimates.

A synthetic mix of the Clague et al. (1991) primary magma estimate was prepared from high-purity elemental oxides and silicates. The mix was ground in an agate mortar under ethyl alcohol for 6 hours to ensure homogeneity. Five hundred milligrams of the ground mix were pressed into a pellet using Elvanol as a binding agent. The pellet was hung on 0.1-mm Pt wire and conditioned in a 1-atm gas mixing furnace at an oxygen fugacity corresponding to the quartz-fayalite-magnetite buffer at 1075 °C for 24 hours. The resulting product was used as starting material for the experiments.

Experiments

Experiments were performed in 1.27-cm piston-cylinder apparatus, similar to the design of Boyd and England (1960), using BaCO₃ as

the pressure medium. For each experiment, 10 milligrams of conditioned starting material were placed in a graphite crucible and welded shut in a Pt outer capsule. The capsule was placed in an alumina sleeve and positioned in the hotspot of a graphite heater with MgO spacers. The heater assembly was loaded into a BaCO₃ pressure cell, which was wrapped with Pb-foil and placed in the pressure vessel. The piston-cylinder apparatus and sample assembly were calibrated for pressure against the transition of anorthite-gehlenite-corundum to Ca-Tschemak's pyroxene as determined by Hays (1965). Temperature was monitored with W₉₇Re₃-W₇₅Re₂₅ thermocouples with no correction applied for pressure. The thermal gradient near the hotspot was measured at 8 °C/mm. Sample thickness is <1.3 mm, resulting in a thermal gradient of <10 °C over its length. Experiments were pressurized at room temperature to 1 GPa, then heated to 865 °C at 100 °C/minute. Experiments were held at 1 GPa and 865 °C for 6 minutes, then pressurized to run pressure and finally heated to run temperature at 50 °C/minute. Experiments were quenched by shutting off the power. Experiments were performed over a pressure range of 1 to 2.2 GPa with a temperature range to constrain the liquidus and subliquidus phase boundaries (Table 2). Experiments above 1.5 GPa were decompressed to 1.0 GPa immediately before quenching to prevent the formation of quench crystals in the liquid regions of the charge (Putirka et al. 1995).

Analytical methods

We analyzed the experimental products by electron microprobe at the Massachusetts Institute of Technology on a JEOL 733 Superprobe using wavelength-dispersive techniques. Data were reduced using the correction scheme of Bence and Albee (1968) with the modifications of Albee and Ray (1970). Crystalline phases in the experiments were analyzed at 15-kV accelerating potential, 10-nA beam current and a spot size on the order of 2 μm. Spot size was increased to 10 μm for glass analyses in order to minimize diffusion of alkali elements away from the region of interest during the analysis. All observed primary phases were analyzed (Table 3). A materials balance calculation was used to estimate the phase proportions (Table 2) and to determine if Fe loss occurred during the experiment. The silicate charge can lose Fe if fractures form in the graphite crucibles and allow the liquid phase to contact the Pt outer capsule. Experiments where the materials balance calculation showed FeO loss of >1% relative were discarded.

Experimental results

Olivine (ol) is the liquidus phase up to ~1.4 GPa (Fig. 1), and low-Ca pyroxene (opx) is on the liquidus at higher pressures. The liquidus is thus cosaturated with the phases present in harzburgite at ~1.4 GPa and ~1425 °C. Below 1.4 GPa, ol crystallization is followed down temperature by opx crystallization. Between 1.4 and 2 GPa, opx crystallization is followed down temperature by ol crystallization, and then by sub-calcic augite (cpx) crystallization. At 1.5 GPa, ol and opx co-crystallize over ~75° of cooling. The appearance of cpx at 1.5 GPa, 1350 °C coincides with the disappearance of ol, which is only found as minor inclusions in opx. A similar crystallization sequence also occurs at 2 GPa, though ol crystallization occurs over a smaller temperature range. The experiment at 2 GPa and 1400 °C has opx, cpx and trace amounts of olivine phenocrysts. Higher temperature 2 GPa experiments only contain opx crystals, and lower temperature experiments only

Table 1 Experimental starting composition and Kilauea tholeiite primary magma estimates ('-' indicates concentration not reported)

Composition	MgO	Al ₂ O ₃	SiO ₂	CaO	TiO ₂	Cr ₂ O ₃	MnO	FeO	P ₂ O ₅	Na ₂ O	K ₂ O	NiO
Estimate based on high-MgO glasses, Clague et al. (1991)												
Experimental starting composition	17.2	10.3	48.8	8.25	1.77	–	0.17	11.6	0.16	1.52	0.27	–
Revised estimates based on high-MgO glasses, Clague et al. (1995)												
High-FeO	18.4	9.83	47.9	7.77	1.66	–	–	12.5	0.17	1.43	0.26	–
Low-FeO	13.4	12.3	51.0	9.72	2.08	–	–	9.13	0.21	1.86	0.33	–
Average	16.5	10.7	49.0	8.55	1.90	–	–	11.2	0.18	1.66	0.30	–
Estimate based on Kilauea Iki lavas, Eggins (1992a)												
Kilauea Iki parent	16.0	10.5	47.8	9.26	2.09	0.13	0.15	11.6	0.20	1.79	0.43	0.10

Table 2 Experimental run conditions and products. (Phase abbreviations: *ol* olivine, *opx* low-Ca pyroxene, *cpx* sub-calcic augite, '-' phase proportions not reported because quench growth in glass prevented quantitative analysis)

Run#	Pressure (Gpa)	Temperature (°C)	Duration (min)	Phases present	Proportions	Σr^2
55	1.00	1450	20	Glass	100	–
56	1.00	1400	40	Glass + ol	93:7	0.2
57	1.00	1350	40	Glass + ol + opx	70:12:18	0.06
38	1.23	1420	270	Glass + ol	98:2	0.2
58	1.50	1480	18	Glass	100	–
59	1.50	1430	38	Glass + opx	96:4	1
61	1.50	1400	16	Glass + ol + opx	–	–
60	1.50	1360	38	Glass + ol + opx	57:4:39	4
62	1.50	1350	40	Glass + opx (w/ol inclusions) + cpx	–	–
34	1.66	1420	720	Glass + opx	77:23	0.2
37	1.71	1450	270	Glass + opx	97:3	0.2
13	1.78	1360	1380	Glass + opx + cpx	44:22:34	0.09
63	2.03	1500	16	Glass + opx	100:trace	–
64	1.98	1450	32	Glass + opx	–	–
65	2.00	1400	126	Glass + ol (trace) + opx + cpx	–	–
11	2.03	1390	1620	Glass + opx + cpx	63:19:18	0.2
9	1.95	1360	3060	Glass + opx + cpx	35:12:53	0.03
147	2.20	1433	276	Glass + opx	93:7	0.1

contain opx and cpx. These results indicate that the ol crystallization field pinches out with increasing pressure, and that above 2 GPa, opx crystallization will likely lead directly to cpx crystallization.

Crystallization along the ol-opx cotectics drives the liquid composition toward the Diopside and Plagioclase apices of the projections (Fig. 2). At 1 GPa, crystallization along this boundary is within the tetrahedron, and saturation with cpx will likely occur within the projection tetrahedron. At higher pressures, the ol-opx cotectic shifts toward the Olivine-Diopside-Plagioclase plane due to the increasing proportion of opx in the crystallizing assemblage. At 1.5 GPa, ol-opx crystallization drives the liquid across the Olivine-Diopside-Plagioclase plane, analogous to crossing the *critical plane of silica undersaturation* of Yoder and Tilley (1962), and cpx saturation likely occurs at negative Quartz values. As pressure increases, the inferred ol-opx-cpx saturation boundary also moves to increasingly higher Olivine values.

Discussion

The contradiction in the inferred mineralogy of the Kilauea magma source

The mineralogy of the Kilauea magma source has principally been inferred from geochemical studies of the rare earth element (REE) abundances of tholeiitic eruptives, and also from experimental studies of the primary magmas that produced these eruptives. Inversion modeling of REE abundance data has shown that Kilauea tholeiites (Budahn and Schmitt 1985), and Hawaiian tholeiites in general (Frey and Roden 1987), formed in equilibrium with garnet and clinopyroxene. Other, more direct evidence for residual garnet is the lack of variation in garnet-compatible element abundances, with concomitant variation in incompatible elements, displayed by cogenetic, tholeiitic lavas from Kilauea (Hofmann et al. 1984). Similar chemical variation was observed in the picroitic Kilauea glasses used to

Table 3 Composition of experimental run products. Uncertainty, 1 standard deviation reported. Phase abbreviations as in Table 2. (–) indicates concentration not reported, # indicates number of analyses

Phase #	MgO un- cer- tainty	Al ₂ O ₃	SiO ₂	CaO	TiO ₂	Cr ₂ O ₃	MnO	FeO	P ₂ O ₅	Na ₂ O	K ₂ O	Total		
BPC-9	9.8	14.48	45.3	9.0	3.6	0.1	0.00	0.15	0.05	13.8	0.1	0.48	0.02	100.0
Opx 5	26.6	0.4	52.2	2.1	0.1	0.44	0.06	0.01	0.10	0.05	0.24	0.01	–	100.9
Cpx 4	20.1	0.5	51.3	8.2	0.5	0.74	0.06	0.05	0.15	0.06	0.87	0.04	–	101.0
Glass 8	11.7	0.2	46.6	9.7	3.3	2.4	0.1	0.07	0.04	0.20	0.03	12.7	0.2	99.5
Opx 9	28.7	0.4	54.2	2.6	0.2	0.26	0.04	0.00	0.16	0.01	0.15	0.02	–	100.8
Cpx 8	23.3	0.7	53.4	8.2	0.8	0.37	0.04	0.01	0.15	0.01	0.50	0.06	–	100.9
Glass 9	9.6	0.1	45.4	9.4	0.1	3.08	0.08	0.01	0.01	0.20	0.06	13.1	0.1	98.7
Opx 6	26.9	0.4	52.5	2.1	0.2	0.37	0.08	0.04	0.06	0.16	0.04	11.30	0.07	99.6
Cpx 4	20.0	0.7	50.7	10.5	0.7	0.62	0.09	0.08	0.02	0.16	0.04	9.5	0.3	99.9
Glass 6	13.5	0.2	47.4	10.0	0.1	2.19	0.06	0.02	0.18	0.04	12.2	0.1	0.30	100.1
Opx 5	30.0	0.6	55.2	2.35	0.09	0.22	0.01	0.17	0.01	0.17	0.01	8.8	0.1	100.7
Glass 6	16.82	0.08	49.3	8.3	0.1	1.80	0.04	0.02	0.22	0.03	11.71	0.07	0.22	100.9
Opx 3	32.4	0.1	56.9	1.53	0.09	0.13	0.02	0.11	0.05	0.09	0.05	7.31	0.02	100.3
Glass 6	16.86	0.09	49.7	8.2	0.1	1.79	0.06	0.02	0.20	0.05	11.6	0.2	0.19	101.0
OI 3	47.6	0.5	40.8	0.27	0.02	0.09	0.01	0.07	0.06	0.10	0.04	11.6	0.2	100.7
Glass 7	17.4	0.1	48.8	7.8	0.2	1.74	0.03	0.01	0.11	0.03	11.3	0.1	0.21	99.4
Glass 7	15.1	0.1	49.5	8.5	0.1	1.88	0.03	0.01	0.12	0.05	11.32	0.08	0.20	99.2
OI 5	47.5	0.3	39.9	0.28	0.00	0.04	0.03	0.00	0.14	0.02	12.03	0.16	0.01	100.1
Glass 7	9.3	0.5	48.9	10.8	0.2	2.44	0.05	0.01	0.02	0.19	0.06	11.6	0.2	99.8
OI 4	44.8	0.2	39.2	0.39	0.00	0.11	0.01	0.10	0.01	0.10	0.01	16.36	0.08	101.1
Opx 6	30.7	0.4	55.1	2.3	0.2	0.38	0.03	0.06	0.02	0.16	0.01	9.4	0.1	101.1
Glass 6	16.5	0.2	49.6	8.1	0.4	1.94	0.06	0.00	0.15	0.05	11.3	0.2	0.23	100.5
Opx 4	32.0	0.5	56.0	1.7	0.1	0.26	0.03	0.00	0.08	0.00	7.5	0.2	–	100.3
Glass 5	6.6	1.2	47.0	10.0	0.3	2.7	0.1	0.02	0.03	0.17	0.05	14.2	0.6	99.7
OI 3	44.7	0.3	39.3	0.38	0.01	0.07	0.04	0.01	0.02	0.17	0.00	16.3	0.2	101.2
Opx 4	29.4	0.5	53.9	2.3	0.2	0.37	0.07	0.00	0.14	0.01	9.61	0.09	–	101.1
Glass a	45.2	0.4	39.7	0.37	0.01	0.05	0.05	0.00	0.00	0.11	0.01	14.12	0.01	100.2
Opx 4	31.0	0.5	55.2	2.1	0.2	0.29	0.07	0.00	0.10	0.00	8.7	0.2	–	101.0
Glass a	29.7	0.5	54.5	2.5	0.4	0.31	0.06	0.00	0.11	0.00	9.7	0.1	–	100.7
Cpx 3	25.3	0.8	53.1	6.5	0.8	0.46	0.03	0.00	0.15	0.02	9.4	0.2	–	99.4
Glass 6	16.7	0.9	49.3	8.5	0.3	2.0	0.2	0.01	0.02	0.177	0.07	11.8	0.2	101.5
Opx 3	32.4	1.6	55.9	1.5	0.2	0.4	0.2	0.02	0.01	0.10	0.03	7.3	0.5	101.0
Glass a	29.9	0.1	55.1	2.59	0.08	0.28	0.01	0.00	0.14	0.01	8.77	0.06	–	101.3
Opx 4	46.2	–	40.6	0.52	–	0.13	–	0.00	–	0.10	–	12.9	–	100.7
Opx 3	27.8	0.3	53.2	2.62	0.15	0.43	0.04	0.02	0.01	0.15	0.01	10.3	0.10	101.3
Cpx b	16.06	0.09	48.5	8.55	0.13	1.72	0.05	0.01	0.01	0.09	0.03	11.78	0.13	99.7
Opx 3	31.9	0.7	55.6	1.88	0.29	0.22	0.04	0.01	0.13	0.01	7.95	0.29	–	100.8

^a Glass not analyzed due to presence of quench growth

^b Phase not analyzed

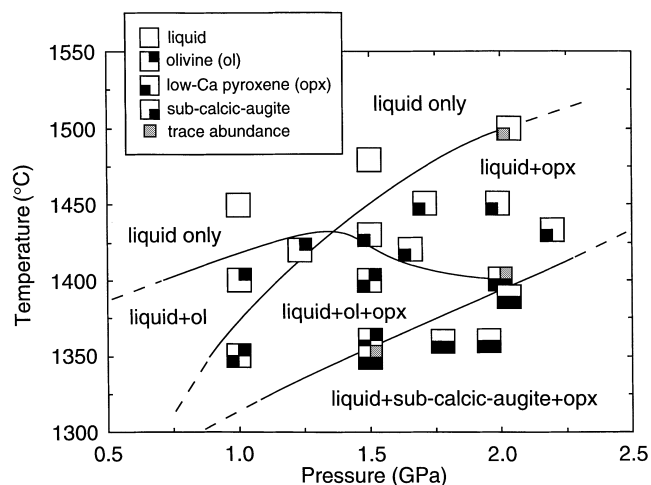


Fig. 1 Pressure-temperature diagram showing the experimental run products and phase boundaries. *Dashed boundaries* are inferred. Highest temperature experiment at 2.0 GPa contains trace amounts of orthopyroxene crystals and is assumed to be near-liquidus

estimate our experimental starting composition (Wagner et al., this issue). The REE abundance data are not sensitive to the presence of olivine and orthopyroxene in the source, but it is assumed that these phases are also present since they are the most refractory phases during lherzolite melting (e.g., Takahashi 1986).

Experimental melting studies, however, show that estimated primary and primitive tholeiites are not in equilibrium with garnet lherzolite on their liquidus at any pressure. Experimental results are often interpreted under the assumption that a primary magma will show cosaturation on its liquidus with the phases present in its residuum at the pressure at which it formed (BVSP 1981). There are good reasons to question the validity of this assumption, as we discuss below. Accepting it for the moment, however, the liquidus relations of primary tholeiites imply that these magmas formed in equilibri-

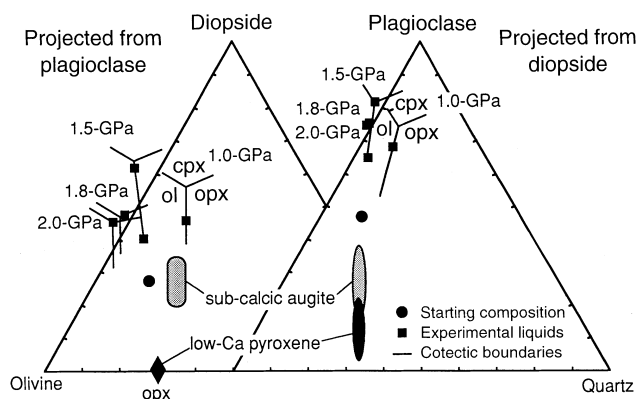


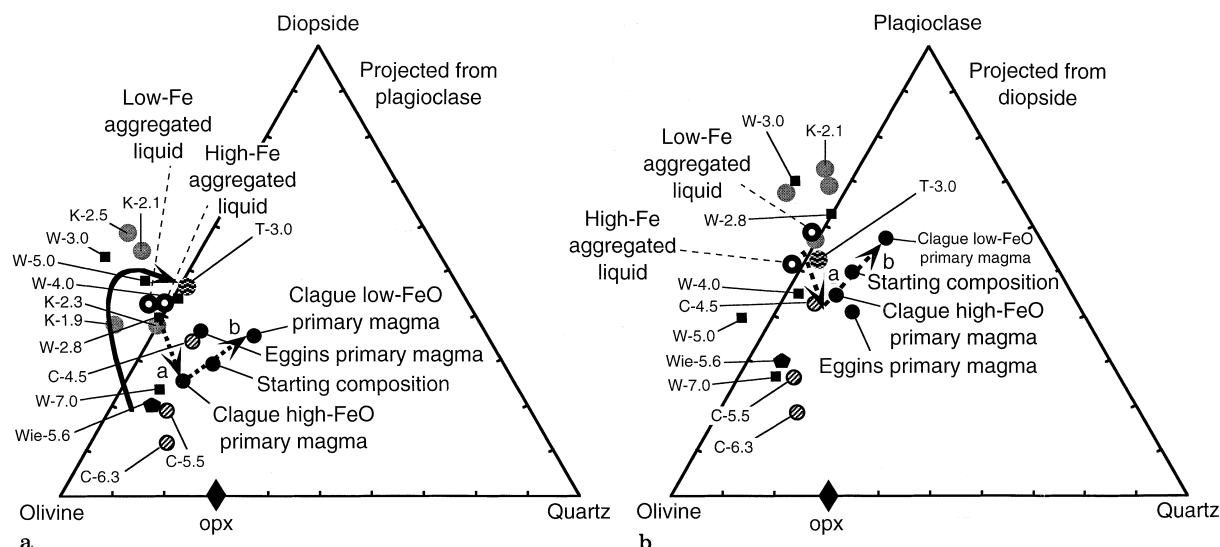
Fig. 2 Ternary projection of experimental liquids and phase boundaries in mineral normative units using the equations of Grove (1993). The 1.0 and 1.8 GPa three-phase saturation boundaries are estimated. At 1.5 and 2.0 GPa, three-phase saturation was achieved within 10 °C of the two-phase saturated experiments plotted (see Table 2)

um only with olivine and orthopyroxene (harzburgite), a much more refractory source than garnet lherzolite. Our starting composition crystallizes olivine on its liquidus to ~ 1.4 GPa, where the liquidus crystallizing phase switches to opx (Fig. 1). Liquidus cosaturation with harzburgite thus occurs at 1.4 GPa. It is important to note that olivine does not crystallize on the liquidus above 1.4 GPa, and disappears as a sub-liquidus phase above 2 GPa (Fig. 1). This pinching out of the olivine field indicates that liquidus cosaturation with lherzolite cannot occur at higher pressures. This conclusion is further supported by the work of Eggins (1992a), on a primary magma estimate based on a Kilauea Iki shield lava. Eggins found that this composition crystallized olivine on its liquidus to ~ 2 GPa, where the liquidus crystallizing phase switched to opx. Clinopyroxene and garnet alternately occurred as liquidus saturating phases at higher pressures, but as in our study, olivine was not a stable liquidus or subliquidus phase, and lherzolite saturation did not occur at any pressure. The higher pressure of harzburgite saturation in the Eggins study was likely due to the lower SiO_2 content of the starting composition.

Possible causes of the contradiction

Why, then, do tholeiite primary magma estimates fail to reach cosaturation on their liquidus with phases present in garnet lherzolite? A possible explanation is the lack of dissolved H_2O in the experiments. The addition of H_2O to basalt-peridotite systems expands the olivine phase volume to higher pressures (Kushiro 1972), and also expands the clinopyroxene and garnet phase volumes to lower pressures (Gaetani and Grove 1993, 1994). The silicate liquid in their experiments, however, contained >6 wt% H_2O , while the high-MgO glasses show that primary tholeiite contains ~ 0.35 wt% H_2O (Clague et al. 1991). Consequently, the incorporation of appropriate amounts of H_2O into our experimental study will likely result in a slight increase in the pressure of liquidus cosaturation with olivine-opx, but will not result in liquidus cosaturation with garnet lherzolite.

Another possibility is that the assumption that the liquidus will be cosaturated with the phases present in the residuum is invalid for magmas generated at Kilauea. If magmas are produced by near-fractional melting, melts are likely produced over a range of depths and continuously extracted in small increments, similar to the production of mid-ocean ridge basalt (e.g., McKenzie and Bickle 1988). If Kilauea primary magmas are aggregates of these polybaric melts, their liquidus relations will depend on the variation in melt composition over the depth range of melting. If melt composition varies along a curved trajectory in compositional space, aggregated melts would not be expected to show multiple saturation with all phases present in the residuum (Klein and Langmuir 1987). The available experimental data on the composition of garnet lherzolite melts show



considerable variability (Fig. 3), though there is some indication that melt composition does form a curved trajectory. The geometric predictions of O'Hara (1968) and the experiments of Walter and Presnall (1994) suggest that melts of garnet lherzolite are nepheline normative at low pressures, but decrease in their normative nepheline contents and eventually cross the Olivine-Diopside-Plagioclase planet at higher pressures. If lower-pressure, higher-degree melts of garnet lherzolite are near this plane, like the 3 GPa experiment of Takahashi (1986), the composition of melts produced by near-fractional decompression melting of a mantle plume could form a curved trajectory convex relative to the Quartz apex (shown schematically as the solid arrow in Fig. 3a). An aggregate of melts along this curve would not be similar in composition to any melt at a single pressure, and the aggregate would not show cosaturation on its liquidus with the phases present in garnet lherzolite. The aggregated melt would, in fact, only be liquidus cosaturated with olivine and opx, similar to the results of our experiments.

However, even if the boundary is strongly curved, the aggregation process can only play a secondary role in generating tholeiite liquidus signatures. Inspection of Fig. 3 shows that tholeiite primary magmas have greater Quartz contents than all reported garnet lherzolite melt compositions at pressures up to 4.3 GPa, the pressure at which melting begins in the Hawaiian plume according to geophysical models of the Hawaiian swell (Liu and Chase 1989, 1991). Aggregation of any of these melts or even the higher-pressure melts with positive Quartz contents cannot produce the primary magmas. This difference in Quartz content will only increase when the composition of more appropriate, lower-degree melts are determined. The melts plotted in Fig. 3 represent melt fractions of >15%, while geochemical evidence indicates that Hawaiian tholeiites form at melt fractions of <6.5% (e.g., Sims et al. 1995). Lower-degree melts would likely plot further away from the Quartz apex than those depicted, increasing the difference between

Fig. 3a,b Ternary projections of experimentally determined liquids in equilibrium with garnet lherzolite and proposed Kilauea tholeiite primary magma estimates. Mineral normative units as in Fig. 2. Labels in *Letter-# format* correspond to the first initial of the author's name and the pressure of the experiment in GPa. [C Canil (1992), K Kinzler (1995), T Takahashi (1986), W Walter (1997), Wei Wei et al. (1990)]. *Open circles* show compositions of aggregated melts discussed in text. *Solid arrow* in **a** schematically illustrates the variation in composition of garnet lherzolite melts as a function of pressure. *Dashed arrows* schematically show the reaction path for garnet lherzolite melts to become tholeiite primary magma. *Arrow a* shows the effect of opx assimilation. *Arrow b* shows the effect of olivine crystallization. *Primary magma* compositions from Table 1

the Quartz contents of the melts and the estimated primary magmas.

We conclude that the estimated primary magmas for Kilauea tholeiite are too rich in normative Quartz to be batch melts or aggregates of polybaric melts of garnet lherzolite, and infer that some process besides melting takes place during tholeiite formation. This process must enrich the melt in normative Quartz, and cause it to display liquidus cosaturation with harzburgite at pressures corresponding to lithospheric depths beneath Kilauea. We propose that these constraints are consistent with the reaction of garnet lherzolite melts with harzburgite prior to segregation from the mantle.

Resolution of contradiction: melt/harzburgite reaction

Ascent and decompression of a mantle melt leads to changes in the melt's liquidus boundaries. Decompression causes the olivine phase volume to expand (Fig. 2), and results in the melt being nearest saturation with olivine and undersaturated with pyroxene. The melt will also become superheated due to the lowering of its liquidus temperature. If the ascending melt came into contact with harzburgite, the melt would react with it by dissolving orthopyroxene. The energy required for dissolution would be supplied by the crystallization of olivine (Kelemen 1990) and the superheat of the melt.

Field observations of a similar reaction process have been made in the Trinity Peridotite, where dunite is formed at melt pathways surrounded by progressively less depleted peridotites (Quick 1981; Kelemen et al. 1992). Experimental studies of melt-harzburgite interaction by Fisk (1986) and Kelemen et al. (1990a) have shown that the SiO_2 content of the melt increases due to reaction. This result is consistent with the higher normative Quartz contents of tholeiite primary magma estimates relative to garnet lherzolite melts (Fig. 3).

The dashed arrows in Fig. 3a,b schematically illustrate how melt/harzburgite reaction could produce Kilauea tholeiite primary magmas from garnet lherzolite melts. For simplicity, the path has been broken into two component vectors. Starting from an average garnet lherzolite melt, the first component is the assimilation of orthopyroxene which drives the melt composition towards Opx (Arrow a in Fig. 3a,b). The second component is olivine crystallization which drives liquid composition away from the Olivine apex (Arrow b in Fig. 3a,b). The Clague et al. (1991, 1995) and Eggins (1992a) estimated primary tholeiites can all be produced by this reaction.

Compositional constraints on reaction

Major elements

Proportions of reactants. We determined the proportions of reactants by mass balancing orthopyroxene, olivine and polybaric aggregated melts of garnet lherzolite against tholeiite primary magma estimates (Table 4). Orthopyroxene composition is from experiment 37 (Table 3), which is near the temperature and pressure of liquidus cosaturation with olivine and orthopyroxene. Olivine composition is $\text{Fo}_{90.7}$. Olivine microphenocrysts of this composition were found in the picritic glass grains, and the Clague et al. (1991) primary magma estimate is in Fe/Mg exchange equilibrium with this olivine. Garnet lherzolite melt composition is difficult to constrain. Initial models, not reported, used melt com-

positions from a single experiment, analogous to a batch melting model, and resulted in poor fits to the data. Subsequent models used aggregated polybaric melts calculated from averages of the experimental melts (Table 4, plotted as open circles in Fig. 3). High-FeO aggregated liquid is an average of the garnet lherzolite melts with the highest-FeO contents: Kinzler 2.1 GPa (Kinzler 1995), Canil 4.5 GPa (Canil 1992) and Walter 5.0 GPa (Walter 1997) (Fig. 3). Low-FeO aggregated liquid was produced by averaging predominantly lower-pressure and lower-FeO melts: Walter 2.8, 3.0 and 4.0 GPa (Walter 1997) and Kinzler 2.1 GPa (Kinzler 1995).

Mass balance was performed by multiple linear regression (Table 4). In all cases, we find that the reaction requires the crystallization of olivine and the assimilation of orthopyroxene, consistent with the phase relations. The MgO , Al_2O_3 and SiO_2 concentrations of the model liquids are remarkably similar to those of the primary magma estimates. The modeled Na_2O and FeO concentrations are lower than those of the primary magma estimates. The mass balance of Na_2O and FeO would likely be improved if more appropriate, lower-degree melts were available because these elements behave incompatibly in the garnet stability field (Walter 1997), the opposite of the behavior of FeO in the spinel stability field (Kinzler and Grove 1993; Baker and Stolper 1995). The CaO contents of the modeled liquids are higher than those of the primary magma estimates. In the spinel stability field, CaO behaves like a compatible element (Kinzler and Grove 1992), and if CaO also behaves compatibly in the garnet stability field, the use of lower-degree melts will improve the CaO mass balance. The CaO contents of experimentally produced melts of garnet lherzolite are too heterogeneous to constrain its behavior, but CaO concentration is correlated with incompatible element abundances in the picritic glasses (Wagner et al., this issue) and Kilauea and Mauna Loa lavas (Frey and Rhodes 1993). This correlation suggests that CaO behaves incompatibly in the garnet stability field, in which case the use of lower-degree melts will not improve the mass balances for CaO. Constraints on the behaviour of CaO await more experimental data.

Table 4 Reaction models. ^AModel used low-FeO aggregated liquid; ^BModel used high-FeO aggregated liquid (Lq liquid, Oliv olivine)

Primary magma estimate	MgO	Al ₂ O ₃	SiO ₂	CaO	FeO	Na ₂ O	Lq	Oliv	Opx	Σr^2
Primary magma estimates and models							Proportions ^{*a}			
Clague et al. (1995), low-FeO Model ^A	13.8	12.6	52.4	9.98	9.33	1.91	85.85	-30.64	44.29	1.2
Clague et al. (1995), high-FeO Model ^B	18.8	10.0	49.0	7.94	12.7	1.46	83.45	-9.12	24.79	9.2
Eggins (1992a) Model ^B	19.1	9.4	49.0	10.0	10.6	1.1	92.33	-16.65	23.54	4.1
	16.5	10.9	49.3	9.55	12.0	1.85				
	16.7	10.3	49.3	10.9	10.8	1.2				
Reactants										
Low-FeO aggregated liquid	17.0	13.2	46.5	11.8	10.0	1.49				
High-FeO aggregated liquid	18.7	10.7	46.4	11.5	11.5	1.26				
Olivine Clague et al. (1991)	49.3	0.00	41.5	0.22	9.03	0.00				
Orthopyroxene This study, exp 37	32.4	1.77	56.9	1.53	7.31	0.08				

^a Proportions determined by multiple linear regression of aggregated liquid, olivine and orthopyroxene against primary magma estimate

Maintaining compositional heterogeneity during reaction.

The variation in FeO content of the primary magma estimates of Clague et al. (1995) indicates that these magmas are likely generated at different mean extents of melting or at different mean depths (Langmuir et al. 1992; Kinzler and Grove 1992, 1993). This compositional variation would be lost if ascending melts came to chemical equilibrium with the surrounding rock during reaction, and the preservation of this signal indicates that melt/rock chemical equilibrium is not achieved. Assimilation without chemical equilibration may be consistent with kinetic constraints. Dissolution rate is only limited by the rate of diffusion in the liquid (Zhang et al. 1989), while chemical equilibrium is rate limited by solid-state diffusion within the surrounding rock. Since solid-state diffusion will be much slower than liquid diffusion, chemical equilibrium will occur at a slower rate than assimilation, and melt compositional variation could be preserved during melt/rock reaction.

Trace elements

The lack of melt/rock chemical equilibrium allows the effect of reaction on melt trace element abundances to be calculated using a simple model of assimilation and fractional crystallization (AFC). We used the AFC equations of DePaolo (1981) to calculate the effect of reaction on the melt's abundances of the high field strength elements (HFSE) Ti and Zr and selected REE (Table 5). Orthopyroxene assimilation can create positive anomalies in the melt's HFSE abundances and decrease its LREE/HREE ratio because orthopyroxene has higher distribution coefficients for the HFSEs and

HREEs relative to adjacent REEs in MORB-based compatibility order (Table 5, Sun and McDonough 1989; Kelemen et al. 1990b). The assimilant for the calculation is an orthopyroxene of constant composition, produced by 20% melting of garnet lherzolite (Table 5). The reacting melt is one of the picritic glasses used in estimation of the experimental starting composition (57-13, Wagner et al., this issue). Technically this glass composition is an inappropriate choice for a reacting melt, since we propose that the glasses come from primary magmas that have already undergone reaction with harzburgite. However, the choice of initial melt composition does not significantly affect the calculation, since all studied trace element abundances are simply diluted by reaction, with little relative fractionation (Table 5).

No significant anomalies in HFSE abundances were produced by either the low- or high-FeO reaction. Zirconium was diluted 0.2 to 0.4% less than the adjacent REE, and Ti showed similar insignificant fractionation. The initial melt has a $Ti/Ti^* = 1.16$, where $Ti/Ti^* = 3Ti/(Eu + 2Dy)$, and there was no significant change in this value for liquids produced by either reaction. Reaction did cause a minor change in the overall slope of the REE pattern. The La/Yb ratio of the initial melt is 3.36, and this decreased by 3% for the low-FeO reaction and 1.8% for the high-FeO reaction. Though the slope change is relatively minor, the difference in post-reaction Yb abundances is potentially significant since Hawaiian eruptives are known to show very little overall variation in Yb abundance. The melt reactions required to produce the high- and low-FeO primary magmas (Table 4) have ratios of mass-assimilated/mass-crystallized that differ by a factor of 2. This variation

Table 5 Effect of melt/harzburgite reaction on melt trace element abundances. *Assimilant* orthopyroxene composition produced by 20% melting of garnet lherzolite, assuming a slightly depleted, chondritic relative source, the melt reaction of Kinzler (1992), and the Ds of Kelemen et al. (1990b) and Hauri et al. (1994a). *F* was calculated as the proportion of final liquid

(Table 4), normalized to the amount of initial liquid. *Ma/Mc* was calculated from the proportions of reactants (Table 4), normalized to the amount of initial liquid. Calculations are not reported for the reaction to produce the Eggins primary magma estimate because it has a similar *Ma/Mc* to the low FeO reaction

Element	Distribution coefficients ^b		Assimilant Orthopyroxene	Initial melt Conc./Cl ^c	Liquid after reaction			
	Olivine	Orthopyroxene			Low-FeO ^c	Δ^d	High-FeO ^c	Δ^d
La	7.00E-06	0.0025	2.57E-10	34.23	29.50	13.8%	29.00	15.3%
Ce	1.00E-05	0.005	3.04E-06	34.23	29.50	13.8%	29.00	15.3%
Nd	7.00E-05	0.01	7.38E-03	29.60	25.52	13.8%	25.09	15.2%
Zr	0.007	0.07	0.34	24.98	21.64	13.4%	21.23	15.0%
Sm	0.0007	0.02	0.10	24.05	20.77	13.6%	20.40	15.2%
Eu	0.001	0.03	0.20	24.05	20.82	13.4%	20.43	15.1%
Ti	0.015	0.15	0.60	22.20	19.32	13.0%	18.93	14.7%
Dy	0.004	0.05	0.38	16.65	14.52	12.8%	14.20	14.7%
Er	0.009	0.07	0.52	14.80	12.97	12.4%	12.66	14.5%
Yb	0.023	0.11	0.73	10.18	9.05	11.1%	8.78	13.7%
Ti/Ti ^a			1.86	1.16	1.16	-0.1%	1.16	-0.2%
La/Yb			3.54E-10	3.36	3.26	3.0%	3.30	1.8%

^a Calculated as $3Ti/(Eu + 2Dy)$

^b Kelemen et al. (1990b)

^c Concentration normalized to C1-chondrite of Anders and Grevesse (1989)

^d Δ is the percentage change in trace element abundance from *Initial melt* to *Liquid* after reaction

produces a 3% difference in post-reaction abundance of Yb. This difference could impart $\pm 1.5\%$ variation in overall Yb abundance, which is well within the $\pm 3\%$ variation reported by A. W. Hofmann for fractionation corrected Hawaiian eruptives.

Thermal energy constraints on reaction

The mass balance calculations (Table 4) show that more orthopyroxene is assimilated than olivine crystallized. Assuming olivine and orthopyroxene have similar latent heats of fusion, an additional source of heat is required to complete the reactions. This excess heat could be in the form of superheat of the ascending melt, the amount of which can be calculated using the mantle solidus and the depth and temperature of melt/rock reaction. The solid line in Fig. 4 shows the solidus for fertile garnet lherzolite from McKenzie and Bickle (1988). Geophysical models of the Hawaiian swell (Liu and Chase 1989, 1991) show that the plume temperature exceeds this solidus and begins to melt at ~ 130 km depth (4.3 GPa). Assuming that melting ends by 2.5 GPa, the stability limit of garnet lherzolite, the plume undergoes 1.8 GPa of decompression melting. Kinzler and Grove (1992) show that 1.8 GPa of decompression melting in the spinel stability field results in a 35°C increase in the solidus, and we assume a similar temperature increase in the garnet stability field. We calculate that plume melts segregating at an average depth of 3.4 GPa would have a mean temperature of 1571°C .

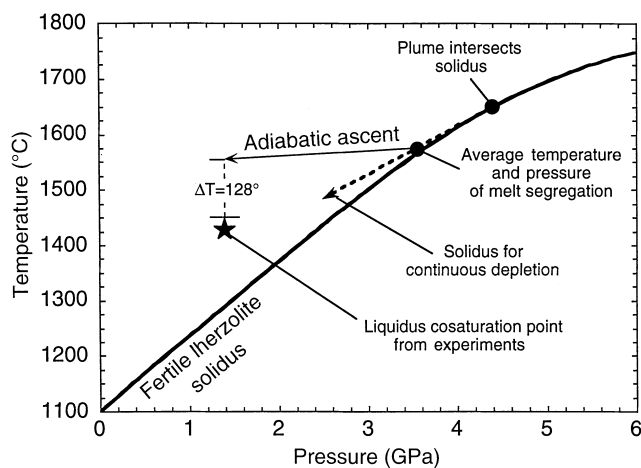


Fig. 4 Mantle solidus beneath Kilauea showing effects of melting and adiabatic ascent on melt temperature. Solidus after McKenzie and Bickle (1988)

The depth and temperature at which melt/harzburgite reaction occurs can be approximated from our experimental results, which show cosaturation on the liquidus with harzburgite at 1.4 GPa and 1425°C (Fig. 1). This cosaturation point may not reflect the actual conditions of reaction, since the melt may not achieve equilibrium with the harzburgite under natural conditions. In this case, the pressure of liquidus cosaturation from the experiments would be greater than the pressure at which reaction actually occurs. Furthermore, if the melt also reacts with harzburgite over a range of depths, experiments on that melt would show liquidus cosaturation with harzburgite at a higher pressure than the mean pressure at which reaction occurred. In any case, the liquidus cosaturation point from the experiments still provides a best estimate of the mean conditions of reaction. During adiabatic ascent from 3.4 to 1.4 GPa, the melt would cool from 1571 to 1553°C , assuming adiabatic ascent cools silicate liquid at 9°C/GPa . The ascended melt would be 128°C above the liquidus cosaturation point temperature of 1425°C (Fig. 4). Using this temperature difference and the proportions of reactants (Table 4), we determined the thermal energy budget of the low- and high-FeO reactions (Table 6). Superheat of the melt alone is greater than the amount of heat required for orthopyroxene assimilation for the high-FeO reaction, and provides more than 75% of the heat required for the low-FeO reaction. There is more than enough heat to complete both reactions when superheat is combined with the latent heat from olivine crystallization.

Where does melt/harzburgite reaction occur?

If magmatism at Kilauea volcano is caused by decompression melting of an upwelling asthenospheric plume, melt/harzburgite reaction could and likely does occur in the top of the plume (Fig. 5a). Ribe and Smooke (1987) suggested that when the plume impinges the lithosphere, melts decouple from the laterally advecting plume solids and continue to ascend vertically. Building on this concept, Eggins (1992b) proposed that garnet lherzolite melts from a large volume of plume material are thus focused through a harzburgite-bearing region in the plume top. The plume top contains harzburgite because the central portion of the plume undergoes more vertical ascent, and hence more melting, than the plume periphery (Fig. 5a). Eggins contended that melts maintain chemical equilibrium with surrounding solids because they segregate by porous flow, and since the melts last

Table 6 Thermal energy budget of reactions. Calculated using proportions of reactants from Table 4 and: C_p of melt = $0.3\text{-cal}/(^\circ\text{C}\cdot\text{g})$; ΔH_f of opx and olivine = $100\text{-cal}/\text{gram}$; $\Delta T = 128^\circ\text{C}$

Reaction	Heat available (cal)		Heat required (cal)	Balance
	Superheat of liquid	Olivine crystallization	Orthopyroxene assimilation	
Low-FeO	+ 3291	+ 3069	-4432	+ 1928
High-FeO	+ 3210	+ 911	-2463	+ 1658

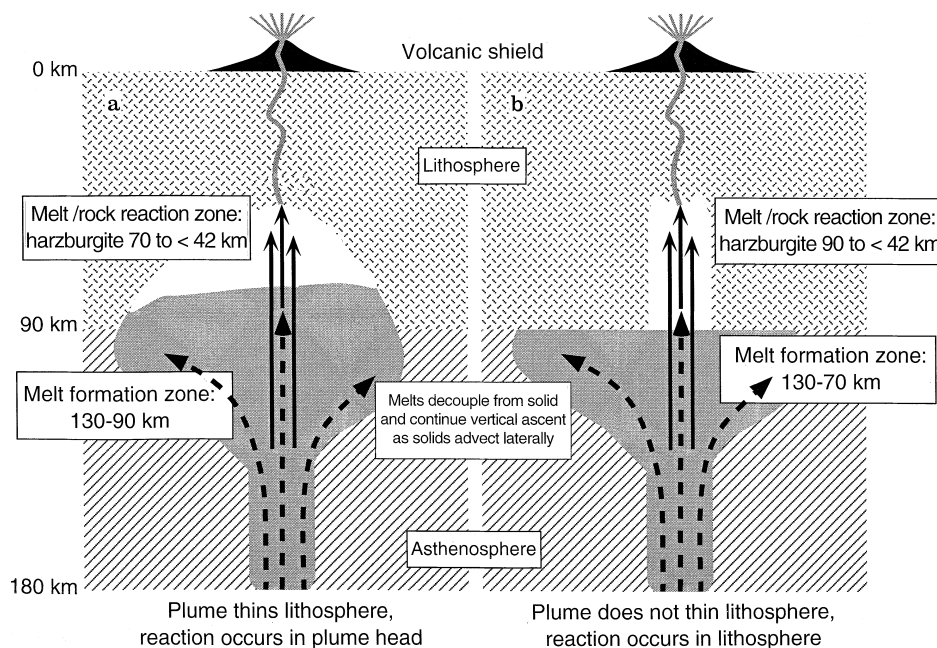


Fig. 5a,b. Formation of Kilauea tholeiite by plume melting and melt/rock reaction, approximately to vertical scale. (*Solid arrows* melt, *dashed arrows* plume solids, *blank fields* zones of harzburgite where melt/rock reaction occurs). Plume is drawn asymmetrically to account for left lateral plate motion. **a** The plume is able to thin the lithosphere. Melts are generated deep in the plume and react with harzburgite in the plume top, similar to Eggins (1992b). The central area of plume undergoes more ascent than the plume periphery, and becomes harzburgite. Assuming 1% melting per 0.1 GPa of decompression (Ahern and Turcotte 1979), decompression melting over a depth range of 130 to 70 km would result in approximately 20% melting of the source. All of the garnet and clinopyroxene in the central area of the plume would thus be consumed, leaving a harzburgite residuum. As the periphery of the plume advects laterally, garnet lherzolite melts continue to ascend vertically and pass through the harzburgite zone (Eggins 1992b; Ribe and Smooke 1987). Melt/rock reaction occurs in the harzburgite at a mean depth of <42 km (see discussion under “Thermal constraints”). Since the lithosphere beneath Kilauea is estimated to be 90-km thick (Detrick and Crough 1978), this model requires the plume to thin more than 48 km of lithosphere. **b** The plume cannot thin the lithosphere. Melts are generated in the plume and react with harzburgite as they ascend through the lithosphere. Reaction occurs over a depth range of 90 km to a mean depth of <42 km. The reaction zone must contain 22–44 wt% orthopyroxene, based on density constraints, assuming the production of 25,000–50,000 km³ of magmas (Frey and Roden 1987) by the average reaction of Table 4. The size of the melt/rock reaction zone was approximated as a cylinder. Cylinder radius is 15 km, corresponding to half of the distance between Kilauea and Mauna Loa, assuming these volcanoes have distinct sources (Frey and Rhodes 1993). Cylinder height is 48 km, corresponding to the vertical distance between the depth/pressure of liquidus cosaturation with olivine-opx from the experiments (42 km, Fig. 1) and the estimated thickness of the lithosphere (90 km)

equilibrate with harzburgite, they show a harzburgite signature in experimental studies.

We concur with the general principles of Eggins’ model, but add to and modify it as follows. First, we propose that the ascending melts move toward chemical equilibrium with the surrounding rock by melt/rock re-

action. Second, we note that ascending melts do not maintain complete chemical equilibrium with the rock through which they ascend, or else the compositional variation observed in primary tholeiite (e.g., Clague et al. 1995) would be lost. Last, we propose that melt/rock reaction is kinetically favored to occur in the plume top, where harzburgite is present, as opposed to deeper parts of the plume, where less refractory materials are present. This effect occurs because reaction rate is limited by the dissolution rate of orthopyroxene, which is a function of the degree of undersaturation of the melt for orthopyroxene (Brearley and Scarfe 1986). During ascent and decompression, the liquidus boundaries of the melt will shift such that the melt will increasingly be undersaturated with respect to orthopyroxene. Hence the rate of melt/rock reaction will be fastest in the plume top, where the plume is composed of harzburgite.

For melt/harzburgite reaction to occur in the plume top, the plume must erode or thin a significant amount of lithosphere. Our experimental results indicate that reaction occurs at a mean depth of 42 km, 48 km into the estimated 90-km thick lithosphere beneath Kilauea (Detrick and Crough 1978). It is not known if such thinning is feasible. Olsen et al. (1988) conclude that significant thinning is not likely based on laboratory experiments. On the other hand, Yuen and Fleitout (1985) and Fleitout et al. (1986) use computer simulations to show that very rapid thinning will occur when secondary convection occurs in the plume top. However, similar studies by Rabinowicz et al. (1990) suggest that secondary convection does not occur.

If, in fact, the plume cannot thin the lithosphere, melt/harzburgite reaction must occur in the lithosphere (Fig. 5b). The lithosphere could contain the requisite amount of orthopyroxene to produce a typically sized Hawaiian shield (Fig. 5b), and the excess thermal energy

from melt superheat (Table 6) could be used thermally to equilibrate the assimilated orthopyroxene in the colder lithosphere. However, studies of Hawaiian lavas and xenoliths do not support melt/harzburgite reaction occurring in the lithosphere during shield tholeiite formation. First, lithospheric xenoliths found in Hawaii are predominantly spinel lherzolite (Sen 1988), not harzburgite or dunite as would be expected if reaction occurred in the lithosphere. Second, trace element and isotopic studies of these xenoliths generally do not indicate interaction with shield tholeiite magmas (Sen et al. 1993; Okano and Tatsumoto 1996). Third, radiogenic isotope ratios of Kilauea and other Hawaiian shield tholeiites do not support interaction between these magmas and a depleted, mid-ocean ridge basalt (MORB) source, as would be present in lithospheric mantle. West et al. (1987) show that Hawaiian tholeiites do not trend toward the Pacific-MORB source in terms of Sr, Nd or Pb isotopes, and Hauri et al. (1994b,c) show that the Os isotopic ratios of Kilauea tholeiites are substantially higher than those of the MORB source.

We conclude that if Hawaiian magmas are produced by decompression melting of an upwelling plume, melt/harzburgite reaction most likely occurs in the plume top and not the lithosphere. Therefore, the plume must be able to thin the lithosphere, possibly by the secondary convection mechanisms proposed by Yuen and Fleitout (1985).

Concluding remarks

We have shown that melt/rock reaction is consistent with phase equilibria, major element, trace element, and thermal constraints on the formation of Kilauea tholeiite. We conclude that melt/rock reaction plays a significant role in the formation of Kilauea tholeiite, and infer that tholeiite forms in a two-stage process. In stage one, melts are generated by decompression melting of garnet lherzolite in a mantle plume. The melts are much poorer in normative silica than tholeiite primary magmas. In stage two, these melts ascend and begin melt/rock reaction with harzburgite by assimilating orthopyroxene and crystallizing olivine. This process increases the magma's normative silica content and dilutes, but does not fractionate, its incompatible trace element abundances. The end product of reaction is a typical tholeiite primary magma. Based on geochemical studies of Hawaiian magmas and xenoliths, it seems likely that melt/harzburgite reaction occurs in the top of the plume. Understanding the evolution of the plume top reaction zone may ultimately help explain the transition between tholeiitic and alkalic volcanism that occurs at the end of the shield building stage of Hawaiian volcanoes.

Acknowledgments T.W. thanks R. Kinzler for teaching him how to do piston-cylinder experiments and helpful discussion, and P. Kelemen and the Keck Marine Geodynamics seminar at the Woods Hole Oceanographic Institution for inspiring him to think about melt/rock reaction. Special thanks go to F. Frey, E. Hauri

and D. Clague for discussion and reviews of earlier versions of the manuscript; E. Takazawa for help with the trace element modeling; and M. Walter for access to preprints and unpublished data. Thanks also go to N. Chatterjee, H. Dick, S. Eggins, G. Gaetani, D. Green, A. Saal, N. Shimizu, and H.J. Yang for helpful discussion. S. Recca and M. Jercinovic assisted with the electron microprobe analyses. This paper was formally reviewed by S. Eggins and G. Sen, who pointed out some of the problems associated with reaction occurring in the lithosphere. This work was supported by the US National Science Foundation.

References

- Ahern JL, Turcotte DL (1979) Magma migration beneath an ocean ridge. *Earth Planet. Sci Lett* 45: 115–122
- Albee AL, Ray L (1970) Correction factors for electron microprobe microanalysis of silicates, oxides, carbonates, phosphates and sulfates. *Anal Chem* 42: 1408–1418
- Anders E, Grevesse N (1989) Abundances of the elements: meteoritic and solar. *Geochim Cosmochim Acta* 53: 197–214
- Baker MB, Stolper EM (1995) Determining the composition of high-pressure mantle melts using diamond aggregates. *Geochim Cosmochim Acta* 58(13): 2811–2827
- Bence AB, Albee AL (1968) Empirical corrections factors for the electron microanalysis of silicates and oxides. *J Geol* 76: 382–403
- Boyd FR, England JL (1960) Apparatus for phase equilibrium studies at pressures up to 50 kbar and temperatures up to 1750 °C. *J Geophys Res* 65: 741–748
- Brearley M, Scarfe CM (1986) Dissolution rates of upper mantle minerals in an alkali basalt melt at high pressure: an experimental study and implication for ultramafic xenolith survival. *J Petrol* 27(5): 1157–1182
- Budahn JR, Schmitt RA (1985) Petrogenetic modeling of Hawaiian tholeiitic basalts: a geochemical approach. *Geochim Cosmochim Acta* 49: 67–87
- BVSP (1981) Basaltic volcanism on the terrestrial planets. Pergamon Press Inc, New York
- Canil D (1992) Orthopyroxene stability along the peridotite solidus and the origin of cratonic lithosphere beneath southern Africa. *Earth Planet Sci Lett* 11: 83–95
- Clague DA, Dalrymple GB (1987) The Hawaiian-Emperor volcanic chain. 1. Geologic evolution. In: Decker RW, Wright TL, Stauffer PH (eds) *Volcanism in Hawaii*, vol 1. US Geol Surv Prof Pap 1350, Denver, pp 5–54
- Clague DA, Weber WS, Dixon JE (1991) Picritic glasses from Hawaii. *Nature* 353: 553–556
- Clague DA, Moore JG, Dixon JE, Friesen WB (1995) Petrology of submarine lavas from Kilauea's Puna Ridge, Hawaii. *J Petrol* 36(2): 299–349
- DePaolo DJ, (1981) Trace element and isotopic effects of combined wallrock assimilation and fractional crystallization. *Earth Planet Sci Lett* 53: 189–202
- Detrick RS, Crough ST (1978) Island subsidence, hotspots, and lithospheric thinning. *J Geophys Res* 83: 1236–1246
- Eggins SM (1992a) Petrogenesis of Hawaiian tholeiites. 1. Phase equilibria constraints. *Contrib Mineral Petrol* 110: 387–397
- Eggins SM (1992b) Petrogenesis of Hawaiian tholeiites. 2. Aspects of dynamic melt segregation. *Contrib Mineral Petrol* 110: 387–397
- Fisk MR (1986) Basalt magma interaction with harzburgite and the formation of high-magnesium andesites. *Geophys Res Lett* 13(5): 467–470
- Fleitout L, Froidevaux C, Yuen D (1986) Active lithospheric thinning. *Tectonophysics* 132: 271–278
- Frey FA (1991) Mantle yields its secrets. *Nature* 353: 500
- Frey FA, Rhodes JM (1993) Intershield geochemical differences among Hawaiian volcanoes: implications for source compositions, melting processes and magma ascent paths. *Philos Trans R Soc London* 342: 121–136
- Frey FA, Roden MF (1987) The mantle source for the Hawaiian islands: constraints from the lavas and ultramafic inclusions. In:

- Menzies M, Hawkesworth C (eds) *Mantle metasomatism*. Academic Press, London, pp 413–463
- Gaetani GA, Grove TL (1993) Effects of H₂O on melting of mantle peridotite at 10 to 15 kbar. *Trans Am Geophys Union* 74: 657
- Gaetani GA, Grove TL (1994) Melting in the sub-arc mantle: the effects of H₂O on primary magmas and the spinel-to-garnet transition. *Mineral Mag* 58A: 301–302
- Green DH (1970) The origin of basaltic and nephelinitic magmas. *Trans Leicester Lit Philos Soc* 64: 28–59
- Green DH, Ringwood AE (1967) The genesis of basaltic magmas. *Contrib Mineral Petrol* 15: 103–190
- Grove TL (1993) Corrections to expressions for calculating mineral components in “Origin of calc-alkaline series lavas at Medicine Lake volcano by fractionation, assimilation and mixing” and “Experimental petrology of normal MORB near the Kane Fracture Zone: 22–25 °N, mid-Atlantic ridge”. *Contrib Mineral Petrol* 114: 422–424
- Hauri EH, Kurz MD, Wagner TP (1994a): Tracing plume-lithosphere interaction beneath Hawaii: constraints from the osmium isotope systematics of Kilauea tholeiites. *Trans Am Geophys Union* 75(44): 723
- Hauri EH, Wagner TP, Kurz MD (1994b) Melt generation and migration beneath Kilauea: constraints from Os isotopes and phase equilibria. *Mineral Mag* 58A: 392–393
- Hauri EH, Wagner TP, Kurz MD (1994c) Melt generation and migration beneath Kilauea: constraints from Os isotopes and phase equilibria. *Mineral Mag* 58A: 392–393
- Hays JF (1965) Lime-alumina-silica. *Carnegie Inst Wash Yearb* 65: 234–236
- Hofmann AW, Feigenson MD, Raczek I (1984) Case studies in the origin of basalt. III. Petrogenesis of the Mauna Ulu eruption, Kilauea, 1969–1971. *Contrib Mineral Petrol* 88: 24–35
- Kelemen PB (1990) Reaction between ultramafic rock and fractionating basaltic magma. I. Phase relations, the origin of calc-alkaline magma series and the formation of discordant dunite. *J Petrol* 31(1): 51–98
- Kelemen PB, Joyce DB, Webster JD, Holloway JR (1990a). Reaction between ultramafic rock and fractionating basaltic magma. II. Experimental investigations of reaction between olivine tholeiite and harzburgite at 1150–1050 °C and 5 kbar. *J Petrol* 31(1): 99–134
- Kelemen PB, Johnson KTM, Kinzler RJ, Irving AJ (1990b). High-field-strength element depletions in arc basalts due to mantle-magma interaction. *Nature* 345(6275): 521–524
- Kelemen PB, Dick HJB, Quick JE (1992) Formation of harzburgite by pervasive melt/rock reaction in the upper mantle. *Nature* 358: 635–641
- Kinzler RJ (1995) Melting of mantle peridotite at pressures approaching the spinel to garnet transition: application to mid-ocean ridge basalt petrogenesis. *J Geophys Res* 102(B1): 853–874
- Kinzler RJ, Grove TL (1992) Primary magmas of mid-ocean ridge basalts. 2. Applications. *J Geophys Res* 97(B5): 6907–6926
- Kinzler RJ, Grove TL (1993) Corrections and further discussion of the primary magmas of mid-ocean ridge basalts, 1 and 2. *J Geophys Res* 98(B12): 22339–22347
- Klein EM, Langmuir CH (1987) Global correlations of ocean ridge basalt chemistry with axial depth and crustal thickness. *J Geophys Res* 92: 8089–115
- Kushiro I (1972) Effect of water on the composition of magmas formed at high pressures. *J Petrol* 13(2): 311–334
- Langmuir CH, Klein EM, Plank T (1992) Petrological systematics of mid-ocean ridge basalts: constraints on melt generation beneath ocean ridges. In: Phipps-Morgan J, Blackman DK, Sinton JM (eds) *Mantle flow and melt generation at mid-ocean ridges*. Am Geophys Union, Washington, DC, pp 183–280
- Liu M, Chase CG (1989) Evolution of midplate hotspot swells: numerical solutions. *J Geophys Res* 94(B5): 5571–5584
- Liu M, Chase CG (1991) Evolution of Hawaiian basalts: a hotspot melting model. *Earth Planet Sci Lett* 104: 151–165
- Maaloe S (1979) Compositional range of primary tholeiite magmas evaluated from major-element trends. *Lithos* 12: 59–72
- McKenzie D, Bickle MJ (1988) The volume and composition of melt generated by extension of the lithosphere. *J Petrol* 29: 625–679
- Murata KJ, Richter DH (1966) The settling of olivine in Kilauean magmas as shown by the lavas of the 1959 eruption. *Am J Sci* 264: 194–203
- O’Hara MJ (1968) The bearing of phase equilibria studies in synthetic and natural systems on the origin and evolution of basic and ultrabasic rocks. *Annu Rev Earth Planet Sci* 4: 69–113
- Okana O, Tatsumoto M (1996) Petrogenesis of ultramafic xenoliths from Hawaii inferred from Sr, Nd, and Pb isotopes. In: Basu A, Hart SR (eds) *Earth processes – reading the isotopic code*. Am Geophys Union, Washington, DC, pp 135–147
- Olsen P, Schubert G, Anderson C, Goldman P (1988) Plume formation and lithosphere erosion: a comparison laboratory and numerical experiments. *J Geophys Res* 93: 15065–15084
- Putirka K, Johnson M, Kinzler RJ, Longhi J, Walker D (1995) Thermobarometry of mafic igneous rocks based on clinopyroxene-liquid equilibria, 0–30 kbar. *Contrib Mineral Petrol* 123(1): 92–108
- Quick JE (1981) Petrology and petrogenesis of the Trinity Peridotite, an upper mantle diapir in the eastern Klamath mountains, Northern California. *J Geophys Res* 86(B12): 11837–11863
- Rabinowicz M, Ceuleneer G, Monnereau M, Rosemberg C (1990) Three-dimensional models of mantle flow across a low-viscosity zone: implications for hotspot dynamics. *Earth Planet Sci Lett* 99: 170–184
- Ribe NM, Smooke MD (1987) A stagnation point flow model for melt extraction from a mantle plume. *J Geophys Res* 92: 6437–6443
- Sen G (1988) Petrogenesis of spinel lherzolite and pyroxenite suite xenoliths from the Koolau shield, Oahu, Hawaii: implications for petrology of the post-eruptive lithosphere beneath Oahu. *Contrib Mineral Petrol* 100: 61–91
- Sen G, Frey FA, Shimizu N, Leeman WP (1993) Evolution of the lithosphere beneath Oahu, Hawaii: rare earth element abundances in mantle xenoliths. *Earth Planet Sci Lett* 119: 53–69
- Sims KWW, DePaolo DJ, Murrell MT, Baldrige WS, Goldstein SJ, Clague DA (1995) Mechanisms of magma generation beneath Hawaii and mid-ocean ridges: uranium/thorium and samarium/neodymium isotopic evidence. *Science* 267: 508–512
- Sun SS, McDonough WF (1989) Chemical and isotopic systematics of oceanic basalts: implications for mantle composition and processes. In: Saunders AJ, Norry MJ (eds) *Magmatism in ocean basins*. Geol Soc London Spec Publ, pp 313–345
- Takahashi E (1986) Melting of a dry peridotite KLB-1 to up to 14 GPa: implications on the origin of peridotitic upper mantle. *J Geophys Res* 91: 9367–9382
- Wagner TP, Clague DA, Hauri EH, Grove TL (this issue) Trace element abundances of high-MgO glasses from Kilauea, Mauna Loa and Haleakala volcanoes, Hawaii. *Contrib Mineral Petrol*
- Walter MJ (1997) Melting of garnet peridotite and the origin of komatiite and depleted lithosphere. Submitted to *J Petrol*
- Walter MJ, Presnall DC (1994) Melting behavior of simplified lherzolite in the system CaO-MgO-Al₂O₃-SiO₂-Na₂O from 7 to 35 kbar. *J Petrol* 35(2): 329–359
- Watson S, McKenzie D (1991) Melt generation by plumes: a study of Hawaiian volcanism. *J Petrol* 32: 501–537
- Wei K, Tronnes RG, Scarfe CM (1990) Phase relations of aluminum-undepleted and aluminum-depleted komatiites at pressures of 4–12 Gpa. *J Geophys Res* 95(B10): 15817–15827
- West HB, Gerlach DC, Leeman WP, Garcia MO (1987) Isotopic constraints on the origin of Hawaiian lavas from the Maui Volcanic complex, Hawaii. *Nature* 330: 216–219
- Yoder HS, Tilley CE (1962) Origin of basaltic magmas: an experimental study of natural and synthetic rock systems. *J Petrol* 3: 342–532
- Yuen DA, Fleitout L (1985) Thinning of the lithosphere by small-scale convective destabilization. *Nature* 313: 125–128
- Zhang Y, Walker D, Leshner CE (1989) Diffusive crystal dissolution. *Contrib Mineral Petrol* 102: 492–513